Appl Phys B (2009) 97: 357–362
DOI 10.1007/s00340-009-3694-6

Applied Physics B
Lasers and Optics

Er,Yb:$YAl_3(BO_3)_4$—efficient 1.5 μm laser crystal

N.A. Tolstik · V.E. Kisel · N.V. Kuleshov · V.V. Maltsev · N.I. Leonyuk

Received: 18 April 2009 / Revised version: 7 July 2009 / Published online: 20 August 2009

Abstract This article summarizes the latest achievements in the growth and characterization of Er,Yb:$YAl_3(BO_3)_4$ laser crystal emitting in the 1.5–1.6 μm spectral range. Fundamental spectroscopic parameters relevant to laser performance of Er,Yb:YAB derived from absorption and emission spectra and from excited state dynamics are presented. The laser performance of Er,Yb:YAB in the cw and mode-locked regimes is reported.

PACS 42.55 Xi · 42.70.Hj · 78.20Ci

1 Introduction

Lasers emitting in the 1.5–1.6 μm spectral range are known since 1962, when Kiss and Duncan have obtained oscillations in an Er-doped $CaWO_4$ crystal [1]. The advantages of the 1.5–1.6 μm spectral range such as comparative eye-safety and high atmosphere transmission were quickly comprehended by research all over the world, mainly for telemetry and laser ranging applications. Soon the first pulsed operation of the Er,Yb:glass laser was reported [2]. Gradually erbium glass had become the most common 1.5 μm active medium due to its excellent spectroscopic properties.

N.A. Tolstik (✉) · V.E. Kisel · N.V. Kuleshov
Institute for Optical Materials and Technologies, Belarusian National Technical University, 65 Nezavisimosti ave., Build. 17, Minsk, Belarus
e-mail: ntolstik@bntu.by
Fax: +375-17-2926286

V.V. Maltsev · N.I. Leonyuk
Geological Faculty, Moscow State University, Moscow 119992/GSP-2, Russia

The energy level structure of the $Er^{3+}-Yb^{3+}$ system is shown in Fig. 1. Ytterbium is usually added to increase the pump absorption efficiency. The pump energy absorbed by Yb ions is transferred to the erbium $^4I_{11/2}$ level, and then in the ideal case relaxed nonradiatively to the $^4I_{13/2}$ level and emitted at 1.5 μm. But the rich energy level structure of the Er^{3+} ion gives rise to a number of excited state absorption (ESA), up-conversion (UC) and cross-relaxation (CR) transitions intensively depopulating the $^4I_{11/2}$ and $^4I_{13/2}$ levels (see Fig. 1). Er→Yb energy back-transfer is also a probable process. Thus the short lifetime of the $^4I_{11/2}$ erbium energy level is a key condition to be fulfilled by an efficient erbium-doped medium. On the other hand, a high 1.5 μm fluorescence quantum yield is necessary to keep a low laser threshold. These contradictory conditions are nicely satisfied in phosphate glasses: the lifetimes of $^4I_{13/2}$ and $^4I_{11/2}$ levels are 8–9 milliseconds and a few microseconds, respectively [3]. As a result the typical slope efficiency of Er,Yb-glass laser is about 20–30% [4].

With the development at the end of 1980s of new InGaAs laser diodes emitting at 980 nm [5] the realization of a cw erbium laser became possible and the requirements for erbium glass have been modified. CW diode-pumped operation of Er:glass laser is limited at several hundred milliwatts of output power mainly due to thermal effects inside the active element intensified by the low thermal conductivity of the glass host. The highest output power obtained to date from a cw diode-pumped bulk Er:glass laser is 353 mW [6]. Crystalline hosts typically exhibit a higher thermal conductivity and can maintain a higher thermal load without destruction.

A number of erbium-doped crystals were investigated in the search for the best active medium for a cw diode-pumped 1.5 μm laser, but typical slope efficiencies were below 10% [8–12], mainly because of a comparatively long $^4I_{11/2}$ level lifetime. Certain progress was demonstrated with

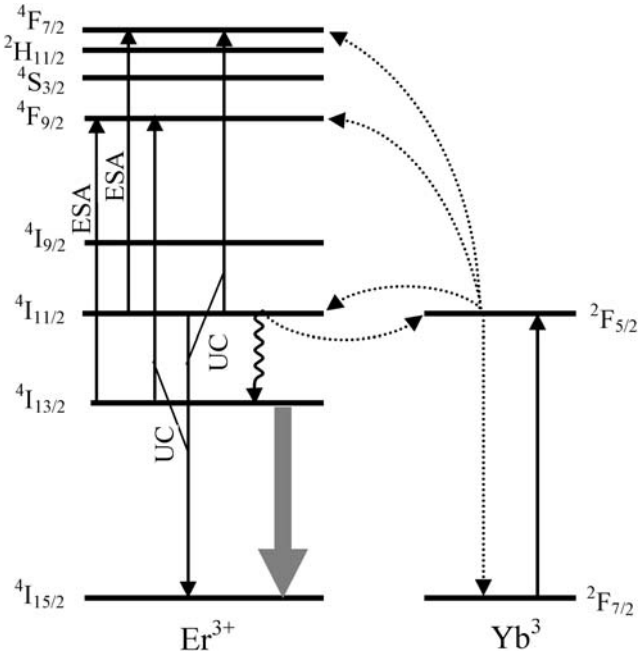

Fig. 1 Energy level structure and main transitions in the Er-Yb-codoped system

Yb,Er-activated $Ca_4YO(BO_3)_3$—270 mW of output power with 26.8% slope efficiency [13]. Borate crystals are characterized by a high phonon energy, which leads to an increased nonradiative decay probability, resulting in short energy level lifetimes. The record performance and output power was achieved with Er,Yb:$YAl_3(BO_3)_4$ crystal (Er,Yb:YAB) introduced recently.

This article will give a comprehensive overview of the spectroscopic and laser properties of Er,Yb:YAB as the best 1.5 μm laser crystal for cw 980 nm diode pumping.

2 Crystal structure and crystal growth

$YAl_3(BO_3)_4$ crystal forms trigonal structure with space group R32. The lattice parameters are: $a = b = 9.293$ Å, $c = 7.245$ Å, $Z = 3$ [14]. Erbium and ytterbium ions substitute for Y^{3+} ions having trigonal prismatic geometry with D_3 point symmetry and surrounded by six oxygen atoms [15]. The Al^{3+} ion occupies the octahedral site, the boron is arranged in sheets of $(BO_3)^{3-}$. This coordination allows for active dopants at the Y^{3+} site to be isolated from one another, which decreases the luminescence quenching effect and allows for high doping levels of active ions [16]. The crystal is a uniaxial anisotropic medium, the refraction indices are equal to 1.7729 for an ordinary wave and 1.6987 for an extraordinary wave at the wavelength of 632.8 nm [17]. YAB is considered to be an excellent self-frequency-doubled crystal being doped either with Nd^{3+} [18] or with Yb^{3+} ions [19]. The density of Yb(7%):YAB is

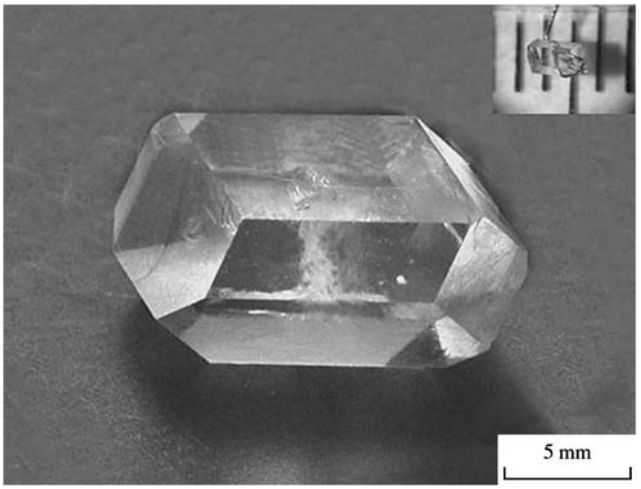

Fig. 2 Er,Yb:YAB single crystal and seed (in the *inset*)

3.844 g/cm^3 [20], the reported thermal conductivity varies from 4.7 W/m K [21] up to 7.7 W/m K [22].

The incongruent melting of YAB requires solution growth techniques. Our crystalline samples were grown by dipping seeded high-temperature solution growth at a cooling rate of 0.2–5°C/day in the temperature range of 1060–1000°C using $K_2Mo_3O_{10}$ based flux. The details of a growth process can be found in [23, 24]. After 30–40 days of growth $15 \times 10 \times 10$ mm^3 Er,Yb:YAB crystals with nicely developed and $\{11\bar{2}0\}, \{2\bar{1}\bar{1}0\}$ and $\{10\bar{1}1\}$ faces were obtained (Fig. 2). The dopant concentrations were measured by microprobe analysis, 1 atomic percent of doping ion is equal to a concentration of 0.55×10^{21} cm^{-3} in YAB. Dopant ions were uniformly distributed over the entire volume of the crystal grown.

3 Spectroscopic properties

Polarized absorption spectra of Er,Yb:YAB crystal measured in the 900–1050 nm range at room temperature with a spectral resolution of 1 nm are shown at Fig. 3 [25]. One can notice comparatively broad (17 nm FWHM) ytterbium absorption band with maximum absorption cross section of about 2.75×10^{-20} cm^2 at 976 nm, which coincides with the emission wavelength of commercial InGaAs laser diodes. The bandwidth is big enough to overlap the diodes emission band.

The emission cross-section spectra can be calculated by the reciprocity method [26].

$$\sigma_{\mathrm{em}}(\lambda) = \sigma_{\mathrm{abs}}(\lambda)\frac{Z_1}{Z_U}\exp\left(\frac{E_{ZL} - hc/\lambda}{k_B T}\right) \quad (1)$$

where $\sigma_{\mathrm{abs}}(\lambda)$ is the polarized absorption cross section, E_{ZL} is the energy gap between the lowest Stark components of

the upper and lower multiplets, k_B is the Boltzmann constant, h is the Planck constant, Z_U and Z_1 are the partition functions of the upper and lower multiplets. The Stark levels were derived from low-temperature absorption and fluorescence spectra measured with high resolution [22] and they are listed in Table 1. Calculated emission spectra as well as experimentally measured fluorescence spectra are plotted in Fig. 4. The spectra look similar with some difference in peak intensities mainly due to reabsorption. The σ-polarized bands are generally stronger than the π-polarized ones and the maximum stimulated emission cross-section is 2.5×10^{-20} cm^2 at 1531.5 nm.

Table 1 Stark levels (cm^{-1}) of Er^{3+} ions in Er:YAB single crystals

Er^{3+}	Sublevel No							
manifold	0	1	2	3	4	5	6	7
$^4I_{15/2}$	0	47	111	125	164	288	306	318
$^4I_{13/2}$	6529	6563	6613	6641	6679	6737	6743	–
$^4I_{11/2}$	10166	10186	10220	10256	10267	–	–	–

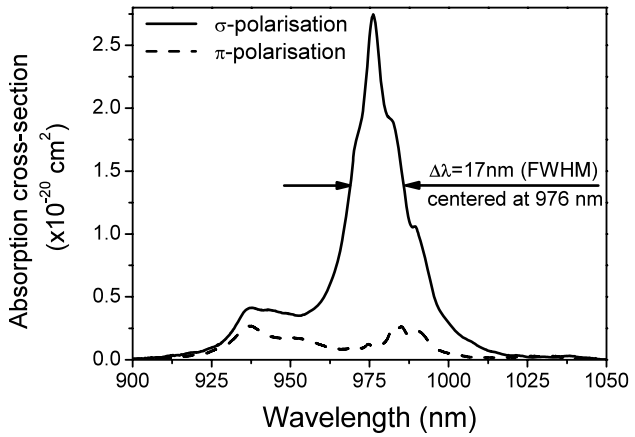

Fig. 3 Room-temperature polarized absorption spectra of Er,Yb:YAB crystal in the 1 μm spectral range

The excited state absorption spectra were measured in the spectral range 1400–1800 nm using the continuous-wave ESA technique [22, 27]. The spectra were calibrated at the spectral region where no ESA is present using ground state absorption and stimulated emission spectra. As shown in Fig. 5, the excited state absorption $^4I_{13/2} \rightarrow {}^4I_{9/2}$ band in YAB starts at 1650 nm and does not overlap with the stimulated emission band.

The fluorescence kinetics were measured using an optical parametric oscillator with 20 ns pulse length as excitation source. The luminescence emission was detected by a fast Ge photodiode or IR photomultiplier tube. Special techniques were used to prevent radiation trapping [28, 29]. The decay curve of 1.5 μm emission was single exponential and the decay time was measured to be about 325 μs, which significantly differs from the value for the radiative lifetime derived from the emission spectra (3.9 ms, [22]) resulting in a 1.5 μm luminescence quantum yield of 8.3%. Such a low luminescence quantum efficiency is explained by the large phonon energy in YAB (>1400 cm^{-1} [30]), which leads to a high non-radiative $^4I_{13/2} \rightarrow {}^4I_{15/2}$ transition probability.

The large phonon energy also affects the erbium $^4I_{11/2}$ level lifetime. This lifetime was estimated by measuring the $^4I_{13/2}$ level rise time at 1.5 μm in Er-single-doped crystal pumped to the $^4I_{11/2}$ level. The measured $^4I_{11/2}$ level lifetime of about 80 ns is much shorter than in any other Er-doped crystal (100 μs in $Y_3Al_5O_{12}$ [7], 16 μs in Y_2SiO_5 [7]), 28 μs in YVO_4 [11]) or even in phosphate glass (2–3 μs, [3]).

The ytterbium $^2F_{5/2}$ level lifetime was measured in Yb-single-doped YAB as well as in Er-Yb-codoped crys-

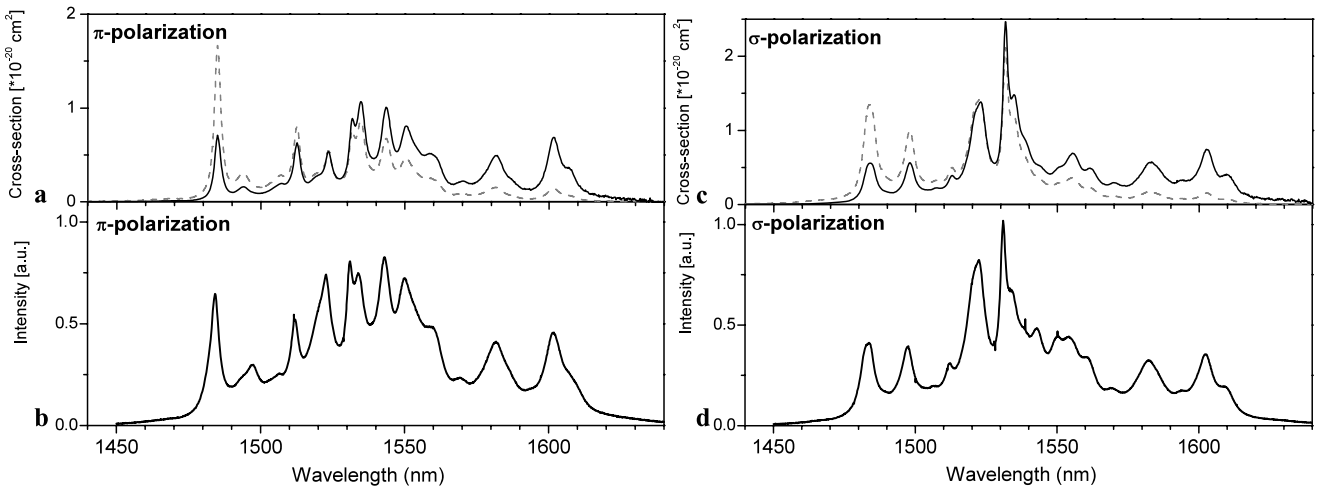

Fig. 4 Absorption spectra (*dashed lines* in (**a**) and (**c**)), derived emission spectra (*solid lines* in (**a**) and (**c**)) and measured luminescence spectra of Er^{3+} in YAB for π (**b**) and σ (**d**) polarizations

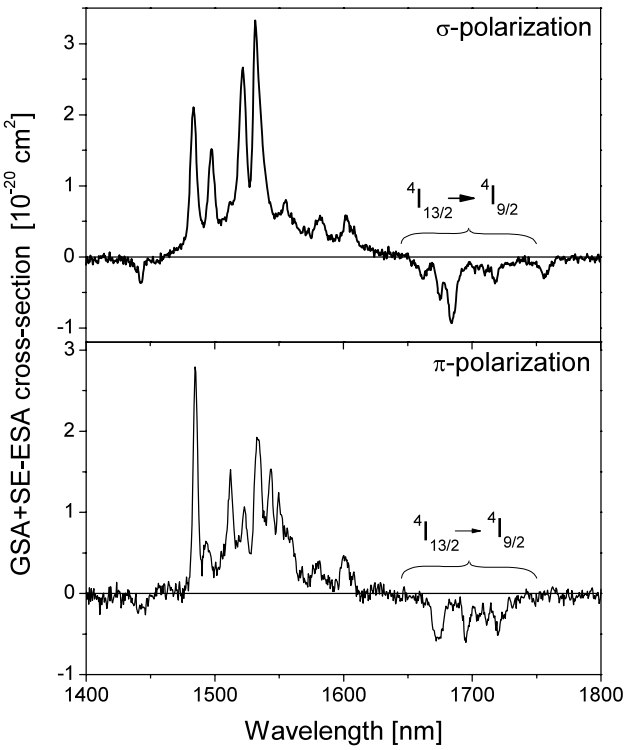

Fig. 5 Room-temperature polarized excited state absorption spectra of Er.Yb:YAB crystal in the 1400–1800 spectral range. The *vertical axis* represents the sum of ground state absorption, stimulated emission and negative excited state absorption cross section

tal. It was found that the lifetime of Yb^{3+} ion shortens from 480 μs in Yb(7at.%):YAB crystal to 60 μs in Er(1.5at.%),Yb(11at.%):YAB. Since the Yb^{3+} concentration rise from 7% to 11% should not affect considerably the $^2F_{5/2}$ level decay [31], the lifetime reduction is a consequence of efficient nonradiative resonant energy transfer from the Yb^{3+} to the Er^{3+} ions. The energy transfer efficiency can be estimated using the simple formula:

$$\eta = k/\tau^{-1} = \tau\left(\frac{1}{\tau} - \frac{1}{\tau_0}\right) \tag{2}$$

where k is the energy transfer rate, τ is the Yb lifetime in Yb,Er-codoped crystal and τ_0 is the Yb lifetime in Yb-single-doped crystal. For Er(1.5%),Yb(11%):YAB crystal the energy transfer efficiency η was determined as high as 88%.

Since the erbium $^4I_{11/2}$ level lifetime in Er,Yb:YAB crystal is very short, energy back-transfer from Er^{3+} to Yb^{3+} ions can be neglected and the Forster–Dexter model of resonant energy transfer can be applied to the system. Energy transfer microparameters were calculated by You et al. [32] to be $c_{da} = 51 \times 10^{-40}$ cm^6 s^{-1} for Yb→Er energy transfer and $c_{dd} = 288 \times 10^{-40}$ cm^6 s^{-1} for Yb→Yb energy migration. These values are higher than the microparameters in phosphosilicate fibers ($c_{da} = 22 \times 10^{-40}$ cm^6 s^{-1} and

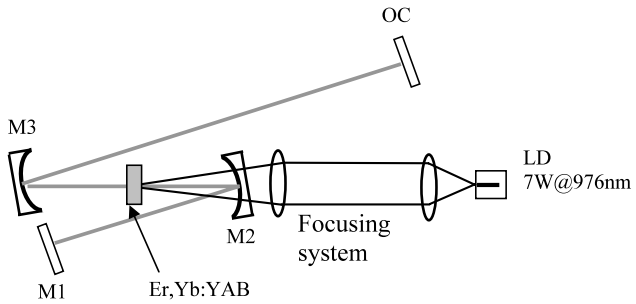

Fig. 6 Cavity configuration used in the laser experiments

$c_{dd} = 175 \times 10^{-40}$ cm^6 s^{-1} [33]). A detailed analysis of the energy transfer dynamics in Er,Yb:YAB crystal will be reported in a separate article.

4 Laser experiments

The first report on the laser action in Er,Yb:YAB crystal is dated June 2006 [34]. Diode-pumped laser experiments performed in a 50-mm hemispherical cavity resulted in 245 mW of cw output power with 16% slope efficiency at 1604 nm. Half a year later Chen et al. have reported quasi-cw lasing with Er,Yb:YAB crystal at 1550 nm [35]. The authors used a pump source with 2% duty cycle to reduce thermal effects inside the crystal, and they have obtained 2 W of peak output power (40 mW of average output power) with a slope efficiency of 21%. In September 2007 quasi-cw lasing was obtained at 1520 nm in the similar experimental setup [36].

In November 2007 diode-pumped cw laser operation of Er,Yb:YAB crystal with 1 W of output power was reported [25]. Laser experiments were performed in a three-mirror folded cavity; the input mirror was deposited onto a surface of a 1.5 mm long c-cut Er(1.5 at.%),Yb(11 at.%):YAB crystal. A 7 W fiber-coupled (∅ = 105 μm, N.A. = 0.22) laser diode emitting near 976 nm was used as a pump source. Maximum output power of 1 W with a slope efficiency of 35% was obtained at 1555 nm. The laser wavelength was found to be dependent on the intracavity passive losses, namely output coupler transmittance, which is typical for three-level lasers.

In order to extend the spectral range of the laser operation and to control the laser wavelength more efficiently a set of spectrally selective output couplers was used. To exclude the influence of thermal effects we applied a four-mirror cavity with active crystal placed in the cavity waist. The cavity consisted of a flat end mirror M1, two folding mirrors M2 and M3 with curvature radii of 100 and 150 mm, respectively, and a flat output coupler (OC). As a pump source the same 7 W fiber-coupled laser diode was used. The pump beam was collimated and then focused by two antireflection-coated 100-mm and 80-mm focal length lenses into 80-μm

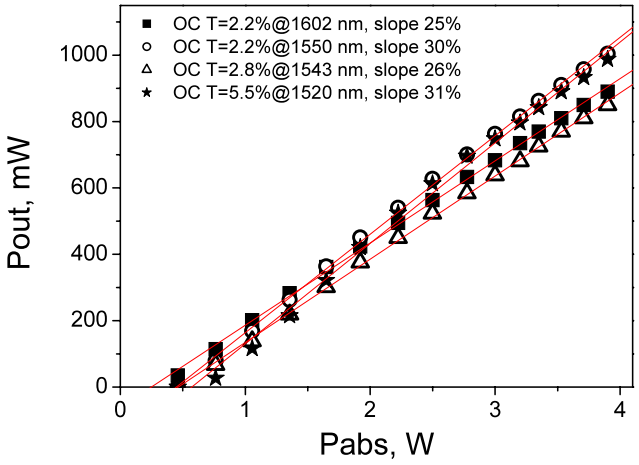

Fig. 7 Output power of cw Er,Yb:YAB laser versus absorbed pump power for different output couplers

spot inside the crystal. The cavity-mode diameter at the active element was also 80 μm. The active element was mounted on a thermoelectrically-cooled heatsink. The cavity setup is presented in Fig. 6.

Laser input-output characteristics are plotted in Fig. 7. The laser action was obtained at four different wavelengths, namely 1602, 1550, 1543 and 1520 nm, depending on the output coupler transmission spectrum. Output couplers were specially designed to suppress lasing at all but the desired wavelengths. The best performance was achieved for OC having 2.2% transmission at 1550 nm: 1 W of output power with 30% slope efficiency. A little less output, 980 mW, was achieved for OC having 5.5% transmission at 1520 nm, and the slope efficiency was estimated as 31%. 850 and 890 mW output power was obtained at the wavelengths of 1543 and 1602 nm, respectively. Laser performance could further be improved by optimization of OC transmittance at the desired wavelength.

Mode-locked laser action with Er,Yb:YAB crystal was reported recently [37]. Laser pulses of 3.8 ps duration with an average output power of 270 mW and 166 MHz frequency were obtained. Er,Yb:YAB is to our knowledge the first erbium-doped crystal which demonstrates passively mode-locked laser operation. Mode-locked laser experiments with high output power are in progress.

5 Conclusion

This article overviews the current results in the research of Er,Yb:YAB—a new promising crystal for 1.5 μm lasers. Full spectroscopic characterization of the crystal is provided including ground state and excited state absorption, stimulated emission, and fluorescence spectra, emission lifetimes, Stark level structure and energy transfer parameters. A brief review of previous laser experiments is presented as well as some novel results. CW laser emission with 0.8–1 W output power is reported at the wavelengths of 1520, 1543, 1550 and 1602 nm.

Acknowledgements We thank Prof. Dr. Guenter Huber and his team for help in low-temperature and excited state absorption spectroscopy.

References

1. Z.J. Kiss, R.C. Duncan, Proc. IREE **50**, 1531 (1962)
2. E. Snitzer, R. Woodcock, Appl. Phys. Lett. **6**, 45 (1965)
3. G. Karlsson, F. Laurel, J. Tellefsen, B. Denker, B. Galagan, V. Osiko, S. Sverchkov, Appl. Phys. B **75**, 41 (2002)
4. P. Laporta, S. Taccheo, S. Longhi, O. Svelto, C. Svelto, Opt. Mater. **11**, 269 (1999)
5. M. Okayasu, T. Takeshita, M. Yamada, O. Kogure, M. Horiguchi, M. Fukuda, A. Kozen, K. Oe, S. Uehara, Electron. Lett. **25**, 1563 (1989)
6. T. Danger, G. Huber, B.I. Denker, B.I. Galagan, S.E. Sverchkov, in *CLEO-98 Conference*, Paper CTuM71
7. T. Schweizer, T. Jensen, E. Heumann, G. Huber, Opt. Commun. **118**, 557 (1995)
8. B. Simondi-Teisseire, B. Viana, A.M. Lejus, J.M. Benitez, D. Vivien, C. Borel, R. Templier, C. Wyon, IEEE J. Quantum Electron. **QE-32**, 2004 (1996)
9. A. Diening, E. Heumann, G. Huber, O. Kuzmin, in *Tech. Dig. CLEO* 1998, p. 299
10. N.V. Kuleshov, A.A. Lagatsky, A.V. Podlipensky, V.P. Mikhailov, A.A. Kornienko, E.B. Dunina, S. Hartung, G. Huber, J. Opt. Soc. Am. B **15**, 1205 (1998)
11. N.A. Tolstik, A.E. Troshin, S.V. Kurilchik, V.E. Kisel, N.V. Kuleshov, V.N. Matrosov, T.A. Matrosova, M.I. Kupchenko, Appl. Phys. B **86**, 275–278 (2007)
12. B. Denker, B. Galagan, L. Ivleva, V. Osiko, S. Sverchkov, I. Voronina, J.E. Hellstrom, G. Karlsson, F. Laurel, Appl. Phys. B **79**, 577–581 (2004)
13. P. Burns, J. Dawes, P. Dekker, J. Piper, H. Jiang, J. Wang, IEEE J. Quantum Electron. **QE-40**, 1575–1582 (2004)
14. D. Mills, Inorg. Chem. **1**, 960 (1962)
15. D. Jaque, M. Ramirez, L. Bausa, J. Garcia Sole, E. Cavalli, A. Speghini, M. Betinelli, Phys. Rev. B **68**, 035118 (2003)
16. P. Wang, J. Dawes, P. Dekker, D. Knowles, J. Piper, B. Lu, J. Opt. Soc. Am. B **16**, 63 (1999)
17. V. Filippov, I. Bodnar, N. Kuleshov, N. Leonyuk, V. Maltsev, O. Pilipenko, J. Opt. Technol. **74**, 717 (2007)
18. B. Lu, J. Wang, H. Pan, M. Jiang, J. Appl. Phys. **66**, 6052 (1989)
19. P. Dekker, P. Burns, J. Dawes, J. Piper, J. Li, X. Hu, J. Wang, J. Opt. Soc. Am. B **20**, 706 (2003)
20. H. Jiang, J. Li, J. Wang, X. Hu, H. Liu, B. Teng, C. Zhang, P. Dekker, P. Wang, J. Cryst. Growth **233**, 248 (2001)
21. J. Blows, P. Dekker, P. Wang, J. Dawes, T. Omatsu, Appl. Phys. B **76**, 289 (2003)
22. N.A. Tolstik, G. Huber, V.V. Maltsev, N.I. Leonyuk, N.V. Kuleshov, Appl. Phys B **92**, 567–571 (2008)
23. N. Leonyuk, V. Maltsev, E. Volkova, O. Pilipenko, E. Koporulina, V. Kisel, N. Tolstik, S. Kurilchik, N. Kuleshov, Opt. Mater. **30**, 161 (2007)
24. O. Pilipenko, V. Maltsev, E. Koporulina, N. Leonyuk, N. Tolstik, N. Kuleshov, Crystallography Rep. **53**, 336 (2008)
25. N.A. Tolstik, S.V. Kurilchik, V.E. Kisel, N.V. Kuleshov, V.V. Maltsev, O.V. Pilipenko, E.V. Koporulina, N.I. Leonyuk, Opt. Lett. **32**, 3233 (2007)
26. D.E. McCumber, Phys. Rev. **136**, A954 (1964)
27. J. Koetke, G. Huber, Appl. Phys. B **61**, 151 (1995)

28. V.E. Kisel, A.E. Troshin, N.A. Tolstik, V.G. Shcherbitsky, N.V. Kuleshov, V.N. Matrosov, T.A. Matrosova, M.I. Kupchenko, Opt. Lett. **29**, 2491–2493 (2004)
29. H. Kuhn, S. Fredrich-Thornton, C. Kraenkel, R. Peters, K. Petermann, Opt. Lett. **32**, 1908 (2007)
30. D. Jaque, M.O. Ramirez, L.E. Bausa, J.G. Sole, E. Cavalli, A. Spheghini, M. Betinelli, Phys. Rev. B **68**, 035118 (2003)
31. J. Liao, Y. Lin, Y. Chen, Z. Luo, E. Ma, X. Gong, Q. Tan, Y. Huang, J. Opt. Soc. Am. B **23**, 2572 (2006)
32. W. You, Y. Huang, Y. Chen, Y. Lin, Z. Luo, Opt. Commun. **281**, 4936 (2008)
33. M. Laroche, S. Girard, J. Sahu, W. Clarkson, J. Nilsson, J. Opt. Soc. Am. B **23**, 195 (2006)
34. N.A. Tolstik, S.V. Kurilchik, V.E. Kisel, N.V. Kuleshov, O.V. Pilipenko, E.V. Koporulina, N.I. Leonyuk, Efficient diode-pumped Er,Yb:YAB laser, in *XII Conference on Laser Optics (LO-2006)*, June 26–30, St. Petersburg, Russia, 2006, paper TuR1-05
35. Y. Chen, Y. Lin, X. Gong, Q. Tan, Z. Luo, Y. Huang, Appl. Phys. Lett. **89**, 241111 (2006)
36. Y. Chen, Y. Lin, X. Gong, Z. Luo, Y. Huang, Opt. Lett. **32**, 2759 (2007)
37. A. Lagatsky, V.E. Kisel, A.E. Troshin, N.A. Tolstik, N.V. Kuleshov, N.I. Leonyuk, A.E. Zhukov, E.U. Rafailov, W. Sibbett, Opt. Lett. **33**, 83–85 (2008)